2011 American Control Conference
on O'Farrell Street, San Francisco, CA, USA
June 29 - July 01, 2011

Adaptive Backstepping PI Sliding-Mode Control for Interior Permanent Magnet Synchronous Motor Drive Systems

Cheng-Kai Lin, Tian-Hua Liu and Li-Chen Fu*

Abstract-**An adaptive backstepping PI sliding-mode control is proposed for speed control of the drive of an interior permanent magnet synchronous motor (IPMSM) subjected to load disturbances. First, a nonlinear model with uncertainties is derived for the IPMSM, and then an adaptive backstepping sliding-mode controller incorporating a linear load torque estimator is designed. Next, the parametric uncertainties of the model are handled with adaptive laws in the design of the controller. To attenuate the chattering problem without sacrificing the feature of the sliding-mode control, an adaptive PI-saturation function is used to approximate the signum function within the boundary layer. Asymptotic stability of the proposed control method is proven by Lyapunov stability theory and Barbalat's lemma. A digital signal processor, TMS320LF2407, is adopted to implement the proposed control scheme. The experimental results show that the proposed system can effectively reduce the chattering phenomenon and has fast transient response, good load disturbance rejection response, and good tracking response.**

I. INTRODUCTION

The interior permanent magnet synchronous motor (IPMSM) has been widely used in industry because of its high efficiency, high torque/ampere ratio, and rugged structure. Several adaptive backstepping sliding-mode controllers have been developed for AC motors or DC motors to increase their control performance [1]-[3]. For example, Lin *et al*. proposed an adaptive backstepping sliding-mode control for linear induction motor drive [1]. The designed control laws can compensate lumped uncertainty in the motion control system. Moreover, an adaptive law was developed to handle the parametric uncertainty in real-time implementation. Shieh and Shyu proposed an adaptive backstepping sliding-mode control for induction motor drives [2]. By using an adaptive backstepping technique, the adverse effect of the unknown but slowly varying parameters in the system can be effectively alleviated. Besides, the proposed method employed the input-output feedback linearization technique; therefore, the nonlinear coordinate transformation is needed to derive the d-q axis control inputs. In [3], an adaptive backstepping controller was proposed to control an IPMSM drive system. The external load torque of the IPMSM was estimated by an adaptive law; however, the performance of the load estimation was not shown in their experimental results. In addition, the convergence of the load estimation error cannot be guaranteed even if the persistent excitation condition is satisfied. The reason is that the external load torque is treated as the external disturbance rather than a parameter of the IPMSM. In the above schemes, excellent dynamic and steady-state performances are shown; however, the systems may suffer chattering due to discontinuous switching functions. To overcome the chattering problem resulting from sliding-mode control, several papers have addressed such an issue [4], [5]. For example, Xu proposed chattering free robust control for nonlinear systems [4]. However, the time-varying feedback gain is very difficult to obtain in real-time implementation. Shahnazi *et al*. proposed a novel adaptive fuzzy PI sliding-mode control for induction and DC servomotors [5]. Through the simulation results, their method indeed showed good tracking performance without chattering.

In this paper, an adaptive backstepping PI sliding-mode control to achieve speed tracking of an IPMSM drive system is proposed. Different from the traditional sliding-mode control, an adaptive PI-saturation function is used to approximate the signum function within boundary layer, which can effectively eliminate chattering. Such results appear to be new in the literature dealing with speed control with IPMSM. In addition, to make the controller more promising for future practical employment, we adopt a DSP to execute the controller, and the experimental results have successfully demonstrated plausibility of the proposed speed control scheme.

II. MODELING OF IPMSM

The nonlinear state equation of an IPMSM in the d-q reference frame can be written as follows [6]:

$$\frac{dx}{dt} = f(x) + g_1 v_d + g_2 v_q \tag{1}$$

where

$$f(x) = \begin{pmatrix} f_1(x) \\ f_2(x) \\ f_3(x) \end{pmatrix} = \begin{pmatrix} -\dfrac{r_s i_d}{L_d} + \dfrac{P_o L_q i_q \omega_{rm}}{L_d} \\ -\dfrac{P_o \omega_{rm} L_d i_d}{L_q} - \dfrac{r_s i_q}{L_q} - \dfrac{P_o \omega_{rm} \lambda_m}{L_q} \\ \dfrac{3P_o i_q \lambda_m + 3P_o (L_d - L_q) i_d i_q}{2J_m} - \dfrac{\omega_{rm} B_m}{J_m} - \dfrac{T_L}{J_m} \end{pmatrix} \tag{2}$$

This work was supported by National Science Council under the grant NSC 97-2221-E-002-178-MY3.

C. K. Lin is with the Department of Electrical Engineering, National Taiwan University, Taipei, Taiwan.
T. H. Liu is with the Department of Electrical Engineering, National Taiwan University of Science and Technology, Taipei, Taiwan.
L. C. Fu is with the Department of Electrical Engineering and Department of Computer Science and Information Engineering, National Taiwan University, Taipei, Taiwan (e-mail: lichen@ntu.edu.tw).

$$x = \begin{pmatrix} x_1 \\ x_2 \\ x_3 \end{pmatrix} = \begin{pmatrix} i_d \\ i_q \\ \omega_{rm} \end{pmatrix},\ g_1 = \begin{pmatrix} 1/L_d \\ 0 \\ 0 \end{pmatrix},\ g_2 = \begin{pmatrix} 0 \\ 1/L_q \\ 0 \end{pmatrix}, \tag{3}$$

where v_d and v_q are d- and q-axis voltages, r_s is stator resistance, i_d and i_q are d- and q-axis currents, L_d and L_q are the d- and q-axis inductances, d/dt is the differential operator, P_o is the number of pole-pairs, ω_{rm} is motor speed, T_L is external load torque, J_m is moment of inertia of rotor, B_m is viscous friction coefficient, and λ_m is flux linkage.

III. Adaptive Backstepping PI Sliding-mode Control

According to (1)-(3) presuming that all the coefficients involved are known only up to some precision level, the dynamic equation of an IPMSM (1) can thus be re-expressed as one subjected to some system uncertainties shown as follows :

$$\frac{dx}{dt} = \left(f_o(x) + \Delta f\,(x)\right) + \left(g_{1o} + \Delta g_1\right)v_d + \left(g_{2o} + \Delta g_2\right)v_q \tag{4}$$

where

$$f_o(x) = \begin{pmatrix} f_{1o}(x) \\ f_{2o}(x) \\ f_{3o}(x) \end{pmatrix} = \begin{pmatrix} -\frac{r_{so}i_d}{L_{do}} + \frac{P_o L_{qo} i_q \omega_{rm}}{L_{do}} \\ -\frac{P_o \omega_{rm} L_{do} i_d}{L_{qo}} - \frac{r_{so} i_q}{L_{qo}} - \frac{P_o \omega_{rm} \lambda_{mo}}{L_{qo}} \\ \frac{3P_o i_q \lambda_{mo} + 3P_o(L_{do} - L_{qo}) i_d i_q}{2J_{mo}} - \frac{\omega_{rm} B_{mo}}{J_{mo}} - \frac{\hat{T}_L}{J_{mo}} \end{pmatrix} \tag{5}$$

$$g_{o1} = \begin{pmatrix} 1/L_{do} \\ 0 \\ 0 \end{pmatrix},\ g_{o2} = \begin{pmatrix} 0 \\ 1/L_{qo} \\ 0 \end{pmatrix} \tag{6}$$

$$\Delta f\,(x) = \begin{pmatrix} \Delta f_1(x) \\ \Delta f_2(x) \\ \Delta f_3(x) \end{pmatrix},\ \Delta g_1 = \begin{pmatrix} \Delta_1 \\ 0 \\ 0 \end{pmatrix},\ \Delta g_2 = \begin{pmatrix} 0 \\ \Delta_2 \\ 0 \end{pmatrix} \tag{7}$$

with the subscript "$_o$" denoting the nominal value of some interested coefficient, $\hat{T}_L$ standing for the estimated external load, Δ symbolizing the system uncertainties including parameter variations and load estimation error, and Δ_1 , Δ_2 representing unknown but bounded constants. Reformulating (4), one can obtain

$$\frac{dx}{dt} = f_o(x) + g_{1o}v_d + g_{2o}v_q + F \tag{8}$$

where

$$F = \begin{pmatrix} F_1 \\ F_2 \\ F_3 \end{pmatrix} = \begin{pmatrix} \Delta f_1(x) + \Delta_1 v_d \\ \Delta f_2(x) + \Delta_2 v_q \\ \Delta f_3(x) \end{pmatrix},\ |F| < \overline{F} = \begin{pmatrix} \overline{F}_1 \\ \overline{F}_2 \\ \overline{F}_3 \end{pmatrix} \tag{9}$$

with $\overline{F}$ being the upper bound of the lumped uncertainty F . Assuming the lumped uncertainty F and the external load T_L are unknown constants. As a result, the lumped uncertainty F and the external load T_L can be approximately estimated by adaptive laws and a load torque estimator, respectively.

A. The External Load Torque Estimator

Assume that the external load torque is an unknown constant and its derivative $\dot{T}_L$ is taken to be zero. For an IPMSM, the system can be described as follows [6]:

$$\begin{bmatrix} \dot{\omega}_{rm} \\ \dot{T}_L \end{bmatrix} = \begin{bmatrix} -\frac{B_{mo}}{J_{mo}} & -\frac{1}{J_{mo}} \\ 0 & 0 \end{bmatrix} \begin{bmatrix} \omega_{rm} \\ T_L \end{bmatrix} + \begin{bmatrix} \frac{3P_o\lambda_{mo}}{2J_{mo}} \\ 0 \end{bmatrix} i_q + \begin{bmatrix} \frac{3P_o(L_{do} - L_{qo})i_d i_q}{2J_{mo}} \\ 0 \end{bmatrix} \tag{10}$$

and

$$y_1 = \omega_{rm} \tag{11}$$

The external load T_L can be estimated using the well-known load torque estimator [6]:

$$\dot{\hat{T}}_L = L_1\left(\dot{\omega}_{rm} + \frac{B_{mo}}{J_{mo}}\omega_{rm} + \frac{1}{J_{mo}}\hat{T}_L - \frac{3P_o\lambda_{mo}}{2J_{mo}}i_q - \frac{3P_o(L_{do} - L_{qo})i_d i_q}{2J_{mo}}\right) \tag{12}$$

where $\hat{T}_L$ is the estimated value, and L_1 is the estimator gain. Unfortunately, in the real implementation, it is difficult to obtain $\dot{\omega}_{rm}$ without high frequency noise. To avoid taking the derivative of the measured speed, a new variable is introduced as

$$x_{c1} = \hat{T}_L - L_1\omega_{rm} \tag{13}$$

Then, it is not difficult to obtain

$$\begin{aligned} \dot{x}_{c1} &= \dot{\hat{T}}_L - L_1\dot{\omega}_{rm} \\ &= L_1\left(+\frac{B_{mo}}{J_{mo}}\omega_{rm} + \frac{1}{J_{mo}}\hat{T}_L - \frac{3P_o\lambda_{mo}}{2J_{mo}}i_q - \frac{3P_o(L_{do} - L_{qo})i_d i_q}{2J_{mo}}\right) \end{aligned} \tag{14}$$

Letting $e_{TL} = T_L - \hat{T}_L$, we can obtain

$$\dot{e}_{TL} = \dot{T}_L - \dot{\hat{T}}_L = \frac{L_1}{J_{mo}}e_{TL} \tag{15}$$

The dynamic behaviour of the estimator can be easily determined by the negative estimator gain L_1 . The estimated load torque is used for the following proposed controller to compensate the load disturbance.

B. Controller Design

The control purpose is to combine the adaptive backstepping sliding-mode control with adaptive PI-saturation function to maintain the speed and the d-axis current along the trajectories with desired performance. Unlike the input-output feedback linearization technique used in [6], the method in this paper does not require any nonlinear coordinate transformation. Besides, the proposed method is more robust than the conventional adaptive backstepping control in [3] due to the fact that the sliding-mode control can effectively compensate for fast varying parameters in the system [5]. However, the discontinuous function (or switching function) is used in the conventional sliding-mode controller; as a result, chattering cannot be avoided. To overcome the chattering phenomenon, a PI-saturation function is used here when the state of sliding surface is within the boundary layer [5]. By suitably adjusting the d-axis current, a MTPA (maximum torque per ampere) characteristic can be achieved. In addition, combination of adaptive backstepping PI sliding-mode controller with external load torque estimator can compensate for the uncertainties caused by the lumped parameter variations, measurement errors, and external load disturbances. Now we define the tracking error variables between the state variables and the reference commands as follows:

$$e_1 = \omega_{rm}^* - x_3 \tag{16}$$

$$e_2 = \dot{\bar{\omega}}_{rm}^* - f_{3o}(x) \tag{17}$$

$$e_3 = i_d^* - x_1 \tag{18}$$

and

$$\dot{\bar{\omega}}_{rm}^* = k_1 e_1 + \dot{\omega}_{rm}^* \tag{19}$$

where k_1 is the closed-loop feedback constant, and $\dot{\bar{\omega}}_{rm}^*$ is the virtual control variable which is to stabilize the acceleration error. To achieve MTPA control, the d-axis current command i_d^* should be expressed as [6]

$$i_d^* = \frac{-\lambda_{mo}}{2(L_{do} - L_{qo})} - \sqrt{\frac{\lambda_{mo}^2}{4(L_{do} - L_{qo})^2} + i_q^2} \tag{20}$$

From (16)-(19), together with (8) and (9), the time derivatives of tracking errors are written as

$$\begin{aligned} \dot{e}_1 &= \dot{\omega}_{rm}^* - \dot{x}_3 \\ &= -k_1 e_1 + e_2 - F_3 \end{aligned} \tag{21}$$

$$\begin{aligned} \dot{e}_2 = &-k_1^2 e_1 - k_1 F_3 + k_1 e_2 + \ddot{\omega}_{rm}^* + (f_{3o} + F_3) M_3 \\ &- M_2 \left(f_{2o} + F_2 + v_q / L_{qo} \right) \\ &- M_1 \left(f_{1o} + F_1 + v_d / L_{do} \right) \end{aligned} \tag{22}$$

$$\dot{e}_3 = \dot{i}_d^* - F_1 - f_{1o} - v_d / L_{do} \tag{23}$$

where

$$M_1 = \frac{3P_o(L_{do} - L_{qo}) i_q}{2J_{mo}},\ M_2 = \frac{3P_o \lambda_{mo} + 3P_o(L_{do} - L_{qo}) i_d}{2J_{mo}},\ M_3 = \frac{B_{mo}}{J_{mo}} \tag{24}$$

The sliding surfaces s_2 and s_3 with the integrated error are chosen as [7]

$$s_q = e_2 + k_{sq} \int_0^t e_2\, dt \tag{25}$$

$$s_d = e_3 + k_{sd} \int_0^t e_3\, dt \tag{26}$$

where k_{sd} and k_{sq} are strictly positive constants. To design the backstepping control scheme, the Lyapunov function with sliding manifold information is selected as

$$V_1 = \frac{1}{2} s_d^2 + \frac{1}{2} s_q^2 \tag{27}$$

Computing the derivative of the Lyapunov function, one can obtain

$$\begin{aligned} \dot{V}_1 &= s_d \dot{s}_d + s_q \dot{s}_q \\ &= s_d \left(\dot{i}_d^* - F_1 - f_{1o} - v_d / L_{do} + k_{sd} e_3 \right) \\ &+ s_q \begin{pmatrix} -k_1^2 e_1 - k_1 F_3 + k_1 e_2 + \ddot{\omega}_{rm}^* + (f_{3o} + F_3) M_3 + k_{sq} e_2 \\ -M_2 \left(f_{2o} + F_2 + v_q / L_{qo} \right) - M_1 \left(f_{1o} + F_1 + v_d / L_{do} \right) \end{pmatrix} \end{aligned} \tag{28}$$

To satisfy $\dot{V}_1 \le 0$, the backstepping sliding-mode control laws are designed as

$$v_d = L_{do} \left(\dot{i}_d^* - f_{m1} + k_d s_d + k_{sd} e_3 + (\bar{F}_1 + \eta_d) \operatorname{sgn}(s_d) \right) \tag{29}$$

$$v_q = \frac{L_{qo}}{M_2} \begin{pmatrix} -M_2 f_{2o} - k_1^2 e_1 + k_1 e_2 + \ddot{\omega}_{rm}^* + f_{3o} M_3 \\ -M_1 f_{1o} - M_1 v_d / L_{do} + k_{sq} e_2 + k_q s_q \\ + \left| M_1 \bar{F}_1 + M_2 \bar{F}_2 + M_3 \bar{F}_3 + k_1 \bar{F}_3 + \eta_q \right| \operatorname{sgn}(s_q) \end{pmatrix} \tag{30}$$

where η_d and η_q are positive constants. Substituting (24) and (25) into (23), one can obtain

$$\dot{V}_1 \le -k_d s_d^2 - k_q s_q^2 - |\eta_d||s_d| - |\eta_q||s_q| \le 0 \tag{31}$$

As one can observe, the derivative of the Lyapunov function is less or equal to zero, and it means that the backstepping sliding-mode control system is stable. However, the upper bounds $\bar{F}_1$, $\bar{F}_2$, $\bar{F}_3$, η_d, and η_q need to be determined. Assume that the lumped uncertainties F_1, F_2, and F_3 can be approximately estimated by adaptive laws under a fixed sampling interval; as a result, the requirement of the knowledge of the upper bounds $\bar{F}_1$, $\bar{F}_2$, and $\bar{F}_3$ can be released. Then, the Lyapunov function can be rewritten as

$$V_2 = V_1 + \frac{1}{2\gamma_1} \tilde{F}_1^2 + \frac{1}{2\gamma_2} \tilde{F}_2^2 + \frac{1}{2\gamma_3} \tilde{F}_3^2 \tag{32}$$

where $\tilde{F}_1 = \hat{F}_1 - \bar{F}_1$, $\tilde{F}_2 = \hat{F}_2 - \bar{F}_2$, $\tilde{F}_3 = \hat{F}_3 - \bar{F}_3$, and γ_1, γ_2, and γ_3 are adaptive gains. The derivative of the Lyapunov function can be expressed as

$$\begin{aligned} \dot{V}_2 &= \dot{V}_1 + \frac{1}{\gamma_1} \tilde{F}_1 \dot{\hat{F}}_1 + \frac{1}{\gamma_2} \tilde{F}_2 \dot{\hat{F}}_2 + \frac{1}{\gamma_3} \tilde{F}_3 \dot{\hat{F}}_3 \\ &= + \frac{1}{\gamma_1} \tilde{F}_1 \dot{\hat{F}}_1 + \frac{1}{\gamma_2} \tilde{F}_2 \dot{\hat{F}}_2 + \frac{1}{\gamma_3} \tilde{F}_3 \dot{\hat{F}}_3 \\ &+ s_d \left(\dot{i}_d^* - F_1 - f_{1o} - v_d / L_{do} + k_{sd} e_3 \right) \\ &+ s_q \begin{pmatrix} -k_1^2 e_1 - k_1 F_3 + k_1 e_2 + \ddot{\omega}_{rm}^* + (f_{3o} + F_3) M_3 + k_{sq} e_2 \\ -M_2 \left(f_{2o} + F_2 + v_q / L_{qo} \right) - M_1 \left(f_{1o} + F_1 + v_d / L_{do} \right) \end{pmatrix} \end{aligned} \tag{33}$$

According to (28), we design the adaptive backstepping sliding-mode control laws v_d and v_q as

$$v_d = L_{do} \left(\dot{i}_d^* - f_{m1} + k_d s_d + k_{sd} e_3 + (\hat{F}_1 + \eta_d) \operatorname{sgn}(s_d) \right) \tag{34}$$

$$v_q = \frac{L_{qo}}{M_2} \begin{pmatrix} -M_2 f_{2o} - k_1^2 e_1 + k_1 e_2 + \ddot{\omega}_{rm}^* + f_{3o} M_3 \\ -M_1 f_{1o} - M_1 v_d / L_{do} + k_{sq} e_2 + k_q s_q \\ + \left(|M_1| \hat{F}_1 + |M_2| \hat{F}_2 + |M_3| \hat{F}_3 + k_1 \hat{F}_3 + \eta_q \right) \operatorname{sgn}(s_q) \end{pmatrix} \tag{35}$$

Substituting (34) and (35) into (33), the following adaptive laws can be obtained

$$\dot{\hat{F}}_1 = \gamma_1 \left(|s_d| + |M_1||s_q| \right) \tag{36}$$

$$\dot{\hat{F}}_2 = \gamma_2 |M_2||s_q| \tag{37}$$

$$\dot{\hat{F}}_3 = \gamma_3 \left(|M_3| + k_1 \right) |s_q| \tag{38}$$

Substituting (34)-(38) into (33), one can satisfy

$$\dot{V}_2 \le -k_d s_d^2 - k_q s_q^2 - |\eta_d||s_d| - |\eta_q||s_q| \le 0 \tag{39}$$

From (39), we can see that the designed adaptive backstepping sliding-mode control can ensure system stability. By increasing the controller gains η_d and η_q in (33) and (34), one can improve the robustness. In fact, larger values of the controller gains η_d and η_q will lead to more chattering in the control inputs. To reduce the chattering, the PI-saturation functions are utilized to approximate the signum functions as

$$\text{PI-sat}(s_i) = \begin{cases} \text{sgn}(s_i), & \text{if } |s_i| > \Phi_i \\ \dfrac{s_i}{\Phi_i} + \Gamma_i, & \text{if } |s_i| \le \Phi_i \end{cases}, \quad i = d,q \tag{40}$$

where

$$\Gamma_i = \gamma_i \int s_i \, dt, \quad i = d,q \tag{41}$$

in which Φ_d and Φ_q are the thicknesses of the boundary layers, and γ_d and γ_q are positive constants. It is assumed that there exist values Γ_d^* and Γ_q^* such that the following inequalities hold when the states stay inside the boundary layers for a finite time [5].

$$\begin{cases} \dfrac{s_i}{\Phi_i} + \Gamma_i^* \ge 1, & \text{for } \dfrac{s_i}{\Phi_i} > 0 \\ \dfrac{s_i}{\Phi_i} + \Gamma_i^* \le -1, & \text{for } \dfrac{s_i}{\Phi_i} < 0 \end{cases}, \quad i = d,q \tag{42}$$

Generally, the optimal values Γ_d^* and Γ_q^* are tuned by trial and error. Therefore, using the adaptive laws to approximate the optimal values is possible under a fixed sampling interval. Consider the following Lyapunov function candidate

$$V_3 = V_2 + \frac{1}{2\gamma_4}\tilde{\Gamma}_d^2 + \frac{1}{2\gamma_5}\tilde{\Gamma}_q^2 \tag{43}$$

where $\tilde{\Gamma}_d = \hat{\Gamma}_d - \Gamma_d^*$, $\tilde{\Gamma}_q = \hat{\Gamma}_q - \Gamma_q^*$, and γ_4 and γ_5 are adaptive gains. The time derivative of (43) can be obtained as

$$\dot{V}_3 = \dot{V}_2 + \frac{1}{\gamma_4}\tilde{\Gamma}_d\dot{\hat{\Gamma}}_d + \frac{1}{\gamma_5}\tilde{\Gamma}_q\dot{\hat{\Gamma}}_q \tag{44}$$

According to (34), (35), and (44), the adaptive backstepping PI sliding-mode control laws v_d and v_q are proposed as

$$v_d = L_{do}\left(\dot{i}_d^* - f_{m1} + k_d s_d + k_{sd} e_3 + (\hat{F}_1 + \eta_d)\rho_d(s_d)\right) \tag{45}$$

$$v_q = \frac{L_{qo}}{M_2}\begin{pmatrix} -M_2 f_{2o} - k_1^2 e_1 + k_1 e_2 + \ddot{\omega}_{rm}^* + f_{3o} M_3 \\ -M_1 f_{1o} - M_1 v_d / L_{do} + k_{sq} e_2 + k_q s_q \\ +\left(|M_1|\hat{F}_1 + |M_2|\hat{F}_2 + |M_3|\hat{F}_3 + k_1\hat{F}_3 + \eta_q\right)\rho_q(s_q) \end{pmatrix} \tag{46}$$

where $\rho_d(s_d)$ and $\rho_q(s_q)$ are defined as

$$\rho_i(s_i) = \begin{cases} \text{sgn}(s_i), & \text{if } |s_i| > \Phi_i \\ \dfrac{s_i}{\Phi_i} + \hat{\Gamma}_i, & \text{if } |s_i| \le \Phi_i \end{cases}, \quad i = d,q \tag{47}$$

Substituting (45)-(47) into (44) and assuming (42) hold, we can rearrange the derivative of the Lyapunov function as

$$\begin{aligned} \dot{V}_3 \le & \frac{1}{\gamma_4}\tilde{\Gamma}_d\left(\dot{\hat{\Gamma}}_d - \gamma_4\left(\eta_d + \hat{F}_1\right)s_d\right) \\ & + \frac{1}{\gamma_5}\tilde{\Gamma}_q\left(\dot{\hat{\Gamma}}_q - \gamma_5\left(\hat{\eta}_q\right)s_q\right) \\ & - k_d s_d^2 - k_q s_q^2 - |\eta_d||s_d| - |\eta_q||s_q| \end{aligned} \tag{48}$$

where $\hat{\eta}_q = \left(|M_1|\hat{F}_1 + |M_2|\hat{F}_2 + |M_3|\hat{F}_3 + k_1\hat{F}_3 + \eta_q\right)$. From (48), the following adaptive laws can be obtained

$$\dot{\hat{\Gamma}}_d = \gamma_4\left(\eta_d + \hat{F}_1\right)s_d \tag{49}$$

$$\dot{\hat{\Gamma}}_q = \gamma_5\hat{\eta}_q s_q \tag{50}$$

Substituting (49) and (50) into (48), one can obtain

$$\dot{V}_3 \le -k_d s_d^2 - k_q s_q^2 - |\eta_d||s_d| - |\eta_q||s_q| \le 0 \tag{51}$$

Since $\dot{V}_3$ is negative semidefinite, it implies s_d, s_q, $\tilde{F}_1$, $\tilde{F}_2$, $\tilde{F}_3$, $\tilde{\Gamma}_d$, and $\tilde{\Gamma}_q$ are bounded. By integrating (51), we can get

$$\begin{aligned} & \int_0^\infty \left(k_d s_d(\tau)^2 + k_q s_q(\tau)^2\right)d\tau \\ & \le -\int_0^\infty \dot{V}_3(\tau)d\tau = V_3(0) - V_3(\infty) < \infty \end{aligned} \tag{52}$$

From (52), we can guarantee that $s_d, s_q \in L_2$. It is not difficult to check that $\dot{s}_d$ and $\dot{s}_q$ are also bounded. Combining the previous results and using Barbalat's lemma, we get the following

$$\lim_{t\to\infty} s_d(t) = 0 \tag{53}$$

$$\lim_{t\to\infty} s_q(t) = 0 \tag{54}$$

From (53) and (54), we can conclude that the closed-loop system is asymptotically stable even if the lumped parameter uncertainties, external load disturbances, and estimation errors exist. Note that (53) and (54) do not imply that the estimated errors $\tilde{F}_1$, $\tilde{F}_2$, $\tilde{F}_3$, $\tilde{\Gamma}_d$ and $\tilde{\Gamma}_q$ will approach zero without satisfying the persistent excitation condition. The closed-loop system is globally asymptotically stable for tracking desired trajectories if the optimal values Γ_d^* and Γ_q^* in (42) hold [5]. To apply the proposed control scheme, the reference commands $\dot{i}_d^*$, $\dot{\omega}_{rm}^*$, and $\ddot{\omega}_{rm}^*$ are required. The whole speed control system is shown in Fig. 1, which consists of an adaptive backstepping PI sliding-mode controller, a d-axis command generator with MTPA, a space vector pulse-width-modulation (SVPWM) inverter, an IPMSM, and an external load estimator.

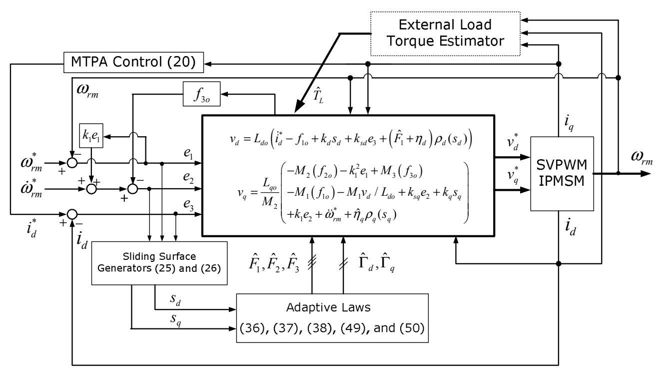

Fig. 1. Computation of the control input voltages.

IV. Experimental Results

A four-pole 750 W three-phase IPMSM, made by the Shin-Ding company, of type 130-750MS-ZK-L2, with rated current 4.2 A is used in this paper. The parameters of the IPMSM are shown in Table I, and the implemented system is shown in Fig. 2. Two phase currents and shaft position of the IPMSM can be measured by Hall-effect sensors and a shaft encoder with resolution of 1024 pulses/rev, respectively. A digital signal processor, TMS320LF2407, is used to implement the adaptive backstepping PI sliding-mode control algorithm written in assemble language. After computing the proposed control algorithm, the d- and q-axis control input voltages can be obtained. According to the computed d- and q-axis voltages, the IPMSM is driven by a three-phase SVPWM inverter with a switching frequency of 4.73 kHz, and the sampling period of the DSP is set as 211 μs. The configuration of the implemented system is shown in Fig. 3, which includes five major parts: A is power supply; B includes two Hall-effect current sensors and two A/D converters; C is DSP board; D is IGBT module; and E includes driver and encoder circuit.

TABLE I
THE PARAMETERS OF IPMSM

P_o	2
r_{so}, Ω	1.9
L_{do}, mH	15.1
L_{qo}, mH	31
λ_{mo}, Vs/rad	0.31
J_{mo} (without load), Kg-m^2	0.0005
B_{mo} (without load), Nms/rad	0.03
J_{mo} (with load), Kg-m^2	0.0227
B_{mo} (with load), Nms/rad	0.0341

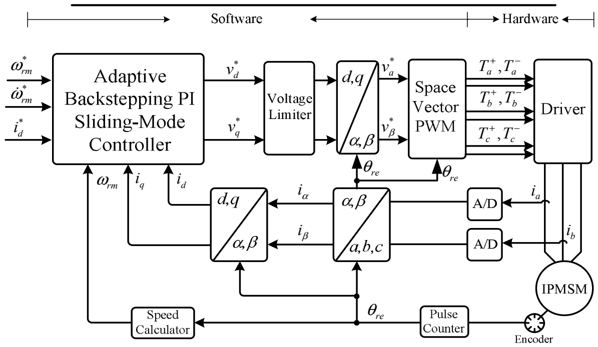

Fig. 2. Implemented system.

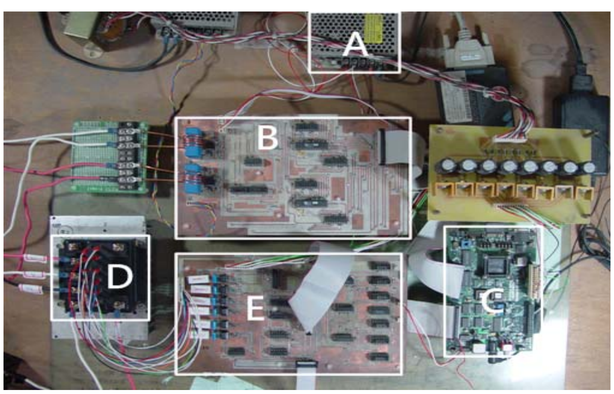

Fig. 3. Circuits of the implemented drive system.

The experiments are conducted with three different test conditions to show and verify the effectiveness of the proposed method and to compare with the traditional adaptive backstepping sliding-mode controllers. In practical experiments, the adaptive backstepping sliding-mode controller and the proposed controller are computed using (34)-(35) and (45)-(46), respectively. The gains for the proposed control scheme are chosen by trial-and-error as $k_1 = 7$, $k_d = 4656$, $k_q = 219$, $\eta_d = 728$, $\eta_q = 93$, $k_{sd} = 72$, $k_{sq} = 289$, $L_1 = -40$, $\Phi_d = 0.03$, $\Phi_q = 12$, $\gamma_1 = 0.167$, $\gamma_2 = 3.21$, $\gamma_3 = 0.4$, $\gamma_4 = 0.00247$ and $\gamma_5 = 0.02473$ to satisfy good performance. Also, the gains for the adaptive backstepping sliding mode controller are the same. Fig. 4(a) and 4(b) show the experimental results of the adaptive backstepping sliding-mode controller and the proposed controller starting with a constant load. As one can observe, when the motor starts with a load of 1.5 Nm, the proposed controller can exhibit good speed tracking performance as the adaptive backstepping sliding-mode controller does. However, compared to Fig. 4(a), there is no chattering observed in Fig. 4(b). Fig. 5(a) and 5(b) show the comparison between the adaptive backstepping sliding-mode controller and the proposed controller at 500 rpm with 2.5 Nm external load torque. The step external load from 0 to 2.5 Nm is added to the IPMSM. It is apparent that the speed can be maintained by the two controllers even though the external load is step-increasing. However, some undesirable chattering in Fig. 5(a) arises from the excessive supplies of the control input voltages. Also, Fig. 5(b) shows that the proposed controller effectively attenuates the chattering of the control input voltages.

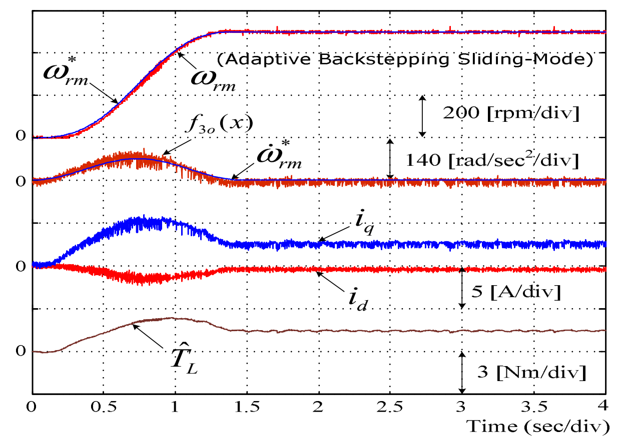

(a)

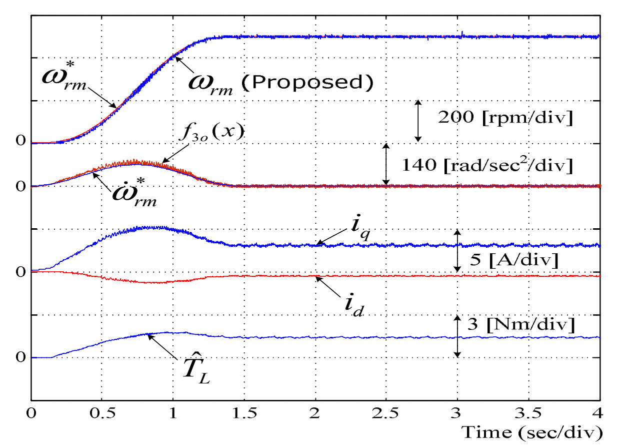

(b)

Fig. 4. Speed response, acceleration response, and d-q axis current responses at 500 rpm with 1.5 Nm load (a) adaptive backstepping sliding-mode control scheme (b) proposed control scheme.

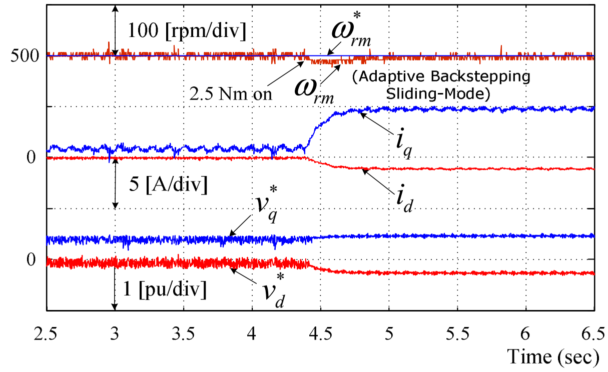

(a)

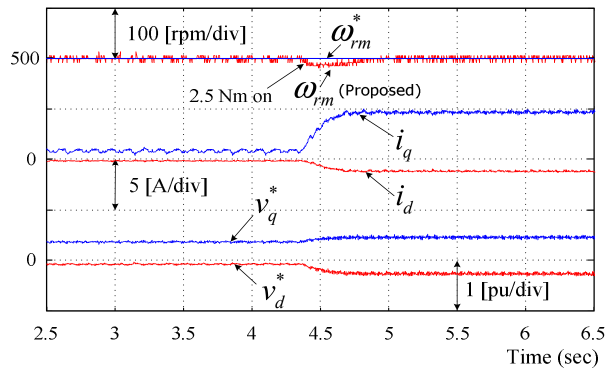

(b)

Fig. 5. Measured results at 500 rpm with 2.5 Nm load applied (a) adaptive backstepping sliding-mode controller (b) proposed controller.

Fig. 6(a) and 6(b) show the experimental results of the two controllers tracking periodic sinusoidal commands. Comparing Fig. 6(a) and 6(b), you can see that the chattering phenomenon of the adaptive backstepping sliding-mode control is removed because of the adaptive PI-saturated functions. Although the adaptive backstepping sliding-mode controller can compensate lumped uncertainties and load disturbances, its switching functions may cause unexpected chattering. From the experimental results, we can conclude that the proposed controller has significantly improved the drawbacks of the adaptive backstepping sliding-mode controller for the IPMSM.

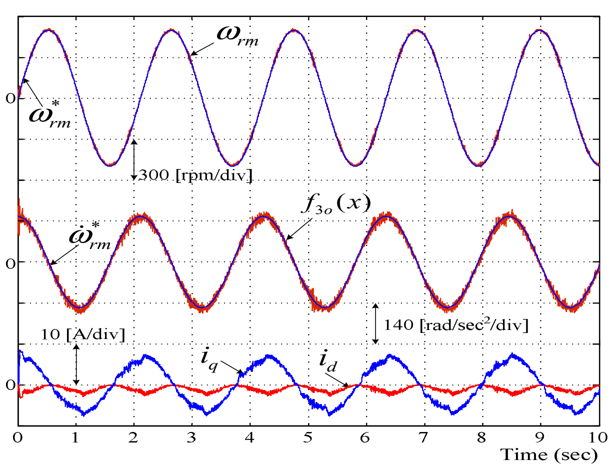

(a)

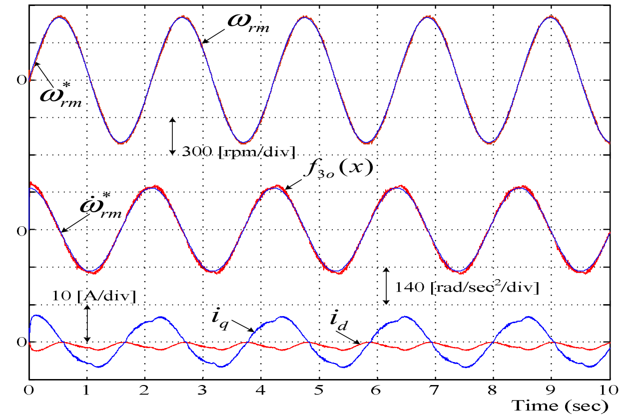

(b)

Fig. 6. Speed response, acceleration response, and d-q axis current responses of periodic sinusoidal-wave command (a) adaptive backstepping sliding-mode control scheme (b) proposed control scheme.

V. Conclusions

In this paper, an adaptive backstepping PI sliding-mode controller is proposed and implemented for an IPMSM speed control system. First, the backstepping sliding-mode technique with available upper bounds of lumped uncertainties is applied to the dynamic model of the IPMSM. To remove the required knowledge of the upper bounds, an adaptive backstepping PI sliding-mode controller with estimation of the lumped uncertainties is proposed. To reduce the chattering, an adaptive PI saturated function is employed to approximate the signum function within boundary layer. Some experiment results show that the proposed system has good transient response, good load disturbance response, and good tracking response.

Acknowledgment

This research was supported by the National Science Council of the Republic of China under grant NSC 97-2221-E-002-178-MY3.

References

[1] F. J. Lin, C. K. Chang, and P. K. Huang, "FPGA-based adaptive backstepping sliding-mode control for linear induction motor drive," *IEEE Trans. Power Electron.*, vol. 22, no. 4, pp. 1222-1231, July 2007.

[2] H. J. Shieh and K. K. Shyu, "Nonlinear sliding-mode torque control with adaptive backstepping approach for induction motor drive," *IEEE Trans. Ind. Electron.*, vol. 46, no. 2, pp. 380-389, Apr. 1999.

[3] M. A. Rahman, D. M. Vilathgamuwa, N. Uddin, and K. J. Tseng, "Nonlinear control of interior permanent-magnet synchronous motor," *IEEE Trans. Ind. Applicat.*, vol. 39, no. 2, pp. 408-416, Mar./Apr. 2003.

[4] Y. Xu, "Chattering free robust control for nonlinear systems," *IEEE Trans. Control Syst. Technol.*, vol. 16, no. 6, pp. 1352-1359, Nov. 2008.

[5] R. Shahnazi, H. M. Shanechi, and N. Pariz, "Position control of induction and DC servomotors: a novel adaptive fuzzy PI sliding mode control" *IEEE Trans. Energy Conver.*, vol. 23, no. 1, pp. 138-147, Mar. 2008.

[6] C. K. Lin, T. H. Liu, and S. H. Yang, "Nonlinear position controller design with input-output linearisation technique for an interior permanent magnet synchronous motor control system," *IET Power Electr.*, vol. 1, no. 1, pp. 14-26, Mar. 2008.

[7] Y. Li and Q. Xu, "Adaptive sliding mode control with perturbation estimation and PID sliding surface for motion tracking of a piezo-driven micromanipulator," *IEEE Trans. Control Syst. Technol.*, vol. 18, no. 4, pp. 798-810, July 2010.